Optical Monitoring of Periodical Structure Formation on Light Metals During a Single Laser Pulse in the Nanosecond Regime

Ignacio Tabares[1*], Marcos Soldera[1], Bogdan Voisiat[1], and Andrés Fabián Lasagni[1,2]

[1] *Institute for Manufacturing Technology, Technische Universität Dresden, George-Baehr-Str. 3c, 01069 Dresden, Germany*
[2] *Fraunhofer Institute for Material and Beam Technology IWS, Winterbergstrasse 28, 01277 Dresden, Germany*
[*]*Corresponding author's e-mail: ignacio.tabares@tu-dresden.de*

Additive manufacturing (AM) is an interesting technique to produce parts with light metal alloys such as Ti-6Al-4V and Scancromal® for aerospace applications. The generated surfaces often require post-processing to improve their quality or be conferred new functionalities. Direct laser interference patterning (DLIP) is a flexible laser-based technique capable of tailoring surface properties by generating structures in the micro/nano range. This study experimentally investigates the dynamics of single-pulse nanosecond DLIP (ns-DLIP) surface structuring on these AM alloys using time-resolved reflectivity measurements. Periodic line-like features with a 6.0 μm spatial period are fabricated by applying single ns laser pulses with fluences ranging from 0.18 to 1.39 J/cm². The material's reflectivity is monitored by analyzing the temporal evolution of the zeroth diffraction order intensity. It is found that the time the material is in the liquid state increases with the pulse fluence, spanning 91 to 154 ns for Ti-6Al-4V and 62 to 115 ns for Scancromal®. By correlating reflectivity variations with structure depths, the growth rates of the periodic features are estimated, reaching maxima of ~35 nm/ns for Ti-6Al-4V and ~50 nm/ns for Scancromal® at the highest fluences investigated. This time-resolved reflectivity approach provides insights into the single-pulse formation dynamics of laser-induced periodic surface structures on these additively manufactured alloys relevant for aerospace applications.

DOI: 10.2961/jlmn.2024.03.2003
Keywords: direct laser interference patterning, time-resolved reflectivity, intra-pulse monitoring.

1. Introduction

Additive manufacturing (AM) techniques have garnered significant attention for industrial applications due to their potential for developing lightweight components with intricate geometries, providing high flexibility in manufacturing processes. Among the various materials that have been used in AM, Al-Cr-Mo-Sc-Zr (Scancromal®) and Ti-6Al-4V alloys demonstrate exceptional strength-to-weight ratios and favorable processability, making them highly suitable for aerospace applications [1-5]. However, additively manufactured parts produced with these materials often necessitate additional surface finishing processes to address surface quality limitations inherent to AM techniques. For instance, the Laser Powder-Bed Fusion (L-PBF) process typically results in surface roughness levels exceeding 5 – 10 μm, which can hinder their direct application. Consequently, post-processing methods are required to enhance the surface quality of these components.

Engineering the topography of a material surface is an adequate way of tailoring its properties in order to achive new functionalities [6-10]. Tailored surfaces can be manufactured by a wide variety of methods including micro-milling, electron and ion beam lithography, and laser-based techniques [11-15]. Direct Laser Interference Patterning (DLIP) stands out as a cost-effective technology among laser-based techniques, capable of producing features in the nano/micro range with diverse geometries and flexibility to tackle an ample range of materials and 3D parts [16,17].

The DLIP process relies on the interference of laser beams to create periodic surface structures by ablating or melting the material at interference maxima positions [18]. For laser sources with pulses in the nanosecond range, DLIP induces local melting of the material, followed by flow and re-solidification [19]. During nanosecond laser pulses, Marangoni convection governs the dynamics of material redistribution. This process takes place when a non-uniform temperature distribution exists in a fluid. Due to the laser intensity contrast in the interference pattern, significant thermal gradients (e.g. over 1000 K/μm) are present between maxima and minima positions, leading to gradients in the surface tension across the molten pool [20,21]. Recoil pressure is another phenomenon that plays an important role when the applied energy density is high enough to produce evaporation in the nanosecond range. The vapor produces a recoil force over the interference maxima positions, pushing the molten material further away to the interference minima [21,22]. At higher intensities, recoil pressure becomes more dominant while the primary mechanism of melt redistribution at lower laser fluence is Marangoni convection [21-24]. Given the complexity of the interplay between the mentioned mechanisms, it is apparent that a deep understanding

of the molten flow dynamics and subsequent topography formation can be exploited for improving the fabrication process and optimize the targeted topography. Although DLIP surface processing with nanosecond pulses has thoroughly been used to treat metallic surfaces [25,26], experimental investigations of the dynamics of the periodical structure formation are scarce. For instance, previous studies on the temporal evolution of the structure formation have mainly focused on semiconductor materials [27,28].

Laser-based surface treatment evaluation methods, including spot probing and coherent scattering, offer avenues for assessing laser-matter interaction processes [29-31]. The use of a reflectivity-based technique offers significant advantages in terms of simplicity, sensitivity to material state changes and ease of application when compared with other strongly proved techniques. Exemplary, methods like pump probing can provide a comprehensive understanding of the dynamics and transcient processes involved in ultrafast laser-material interaction like reported by Fang et al in [32], but its high resolution comes at the expense of highly complex imaging optics and cost-intensitve setups.

Recently, reflectivity-based methods have been successfully employed to monitor structure formation dynamics in semiconductors [33] and stainless steel [34] and can be further applied to AM samples in order to provide better understanding of of structure growth evolution upon single pulse irradiation.

In this study, an improved version of a reflectivity-based method that has previously been applied to stainless steel [34], is utilized to experimentally explore ns-DLIP single pulse processing in additively manufactured Ti-6Al-4V and Scancromal® alloys. These materials have not been only selected because of their widespread use in aerospace applications, but also due to their significant different thermal properties. The method enables the determination of melt and structure formation dynamics, establishing a correlation between reflectivity signal and structure depth evolution during the laser pulse. White light interferometry is used to characterize the fabricated structures, validating the experimental results. Finally, a simple calculation based in the experimental data is presented to determine the temporal evolution and growth rate of the periodic structures as a function of the laser fluence.

2. Experimental

For the purpose of this study, additively manufactured (AM) samples of Ti-6Al-4V and Scancromal® were employed. The titanium-alloy samples were manufactured by Laser Powder Bed Fusion (L-PBF) method, using a DMP flex system (3D Systems, United States) equipped with a 500 W laser in an argon atmosphere. After processing, the material was mechanically polished reaching a roughness S_a of 102 ± 23 nm. The Scancromal® samples were also manufactured by L-PBF method, using an SLM® 125HL system (SLM Solutions Group AG, Germany) under an inert atmosphere. This system employed an ytterbium-YAG fiber laser source, that yielded a maximum laser power of 400 W. The samples were mechanically polished to a roughness S_a of 78 ± 1 nm. Both materials were cleaned with ethanol prior to the laser processing.

Line-like periodic structures were fabricated on the AM samples using Direct Laser Interference Patterning (DLIP) with a diode-pumped solid-state Nd:YAG laser (InnoSlab IS400-3-GH, Edgewave GmbH, Germany) operating at a pulse duration of 6 ns and a fundamental wavelength of 1064 nm. The used optical configuration is shown in Figure 1. The laser beam (LB) propagated through an optical attenuator (AT) and was directed with mirrors into a novel DLIP system (ELIPSYS®, SurFunction GmbH, Germany), where it was split by a diffractive optical element (DOE) into two sub-beams and subsequently shaped by an array of lenses to generate an elongated interference spot with parallel fringes on the sample (S). The spot was approximately elliptical with major *a* and minor *b* axis radii of 1845 µm and 220 µm, respectively.

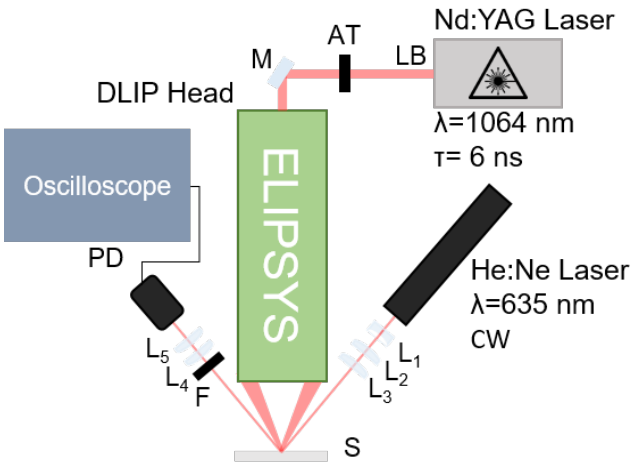

Fig. 1 Experimental ns-DLIP structuring set-up and time-resolved reflectivity configuration.

To calculate the applied laser fluence *F* for a single pulse, the average power *P* of the DLIP-modulated beams at the sample position was measured using a powermeter (FieldMaxII-TO and sensor PM1K+, Coherent, USA) at a laser repetition rate *f* of 5 kHz with varying laser output powers. The pulse energy $E_p = P/f$ was then calculated and the average fluence *F* was determined by considering the elliptical shape of the laser spot as $F = E_p/(\pi \times a \times b)$. The samples were later processed by firing single laser pulses with varying laser fluence starting from 1.39 J/cm² and then decreasing the energy using an attenuator until no signs of ablation were appreciated at the material' surface. For the Ti-6Al-V samples, this value was 0.32 J/cm² and for Scancromal® was 0.18 J/cm². For each fluence level, five individual pulses were used for statistical significance.

Time-resolved reflectivity experiments were conducted with the structuring laser set to a nominal repetition rate of 5 kHz to match the pulse energies used in the laser power measurements. The generated line-like pattern had a spatial period (distance between interference maxima) of 6.0 µm. A control program was written in order to trigger the laser for only a single pulse.

The optical setup assembled for time-resolved reflectivity (TRR) measurements is also shown in Figure 1. The TRR system employed a continuous wave (CW) He:Ne laser (Model 1135, Uniphase, United States) with a central wavelength of 635 nm. The probing laser initially had a circular spot diameter of 690 µm, and 9 mW of power. This beam was expanded by means of a two-lens telescope (L_1 and L_2) and focused by a plano-convex lens with a focal distance of

75 mm to a diameter of ~90 µm into the central region of the processing zone defined by the interference spot dimensions. The laser beam arrived to the sample with an azimuthal angle perpendicular to the pattern fringe direction and with an elevation angle of 45° (see Figure 1).

This geometry avoided the optical axis of the DLIP head and the plasma plume, minimizing possible absorption effects of the He:Ne laser by the plasma plume. The reflected light passed through a narrow-band interference filter (FLH635-10, Thorlabs GmbH, Germany) to suppress the radiation from the Nd:YAG laser and allow only the probe beam radiation through. After the filter, the beam was collected by another lens (L4) and focused using a plano-convex lens (L5, f = 50 mm) onto a Si photodetector (DET025AFC/M, Thorlabs GmbH, Germany). The photodetector signal was acquired by an oscilloscope (Lecroy WavePro W7100A) operating at 1 GHz (with 10 GS/s and 400 ps rise time) set to full bandwith, with as a timebase of 500 ns per division. This enabled 50kS at the mentioned sampling rate, with 100 ps/pt for the total capture time of 5 µs. The oscilloscope was synchronized with the laser controller's trigger to capture the full temporal evolution of the reflectivity for a single pulse. The output signal of the photodiode, representing the relative intensity of the specular reflection (zeroth order of diffraction), was used without normalization. A similar setup has already been reported elsewhere [34, 36]. Its important to notice that this configuration was developed for a spatial period of 6µm, but since it measures only the speculary reflection, it is independent of the structure period as long as the collimating lens is only collecting the zeroth order of diffraction.

The topography of the laser-treated surfaces was measured using white light interferometry (WLI, Sensofar S Neox 3D Surface profiler, Sensofar Metrology, Spain) equipped with a 50x objective, providing a lateral resolution of 0.50 µm and a vertical resolution of 0.1 nm. Measurements of the whole spot were taken, and the resulting images were analyzed using SensoMap 7 software (Sensofar, Barcelona, Spain) to estimate the average structure depth.

3. Results and discussion

3.1 DLIP single pulse structuring and surface characterization of Ti-6Al-V and Scancromal®

The DLIP processing of the Ti-6Al-V samples using a two-beam configuration led to the fabrication of line-like periodic structures with a spatial period of 6.0 µm. Figure 2 shows examples of WLI images of the produced patterns at two different laser fluences. For the Ti-surface shown in Figure 2a, the applied laser fluence was 0.69 J/cm² and it can be observed that the grooves present some irregularities, with discontinuous lines as well as areas where the initial surface roughness is still visible. In addition, the average structure depth was only 180 ± 26 nm. This outcome was in general observed for all Ti-samples treated at low laser fluences, which is typical when metals are treated using ns-pulses [38].

In contrast, at higher laser fluences, the produced line-like patterns (Figure 2b) show a well-defined geometry since at these fluence levels (> 1 J/cm²) the molten material at the maxima positions is displaced towards the minima (due to both Marangoni convection and recoil pressure [21]). For example, the Ti-surface treated at 1.39 J/cm² shows structures with a depth of 659 +/- 57 nm.

From the structure depth measurements, reported in Figure 3, three different structuring regimes can therefore be identified. A first regime where no structure was generated inspite of increasing the fluence (from 0.32 up to ~0.60 J/cm²); then a regime where the line-like structures rapidly become deeper (from 0.69 up to ~0.90 J/cm²); and finally a regime where the structure depth saturates (for fluences over ~ 1.0 J/cm²), at a value of approximately 600 nm. This effect is typical when using single pulses in metals and was explained by the excessive melting of material at the maxima positions due to the high laser power applied, but without an additional contributing to an increase of the structure depth [24,34].

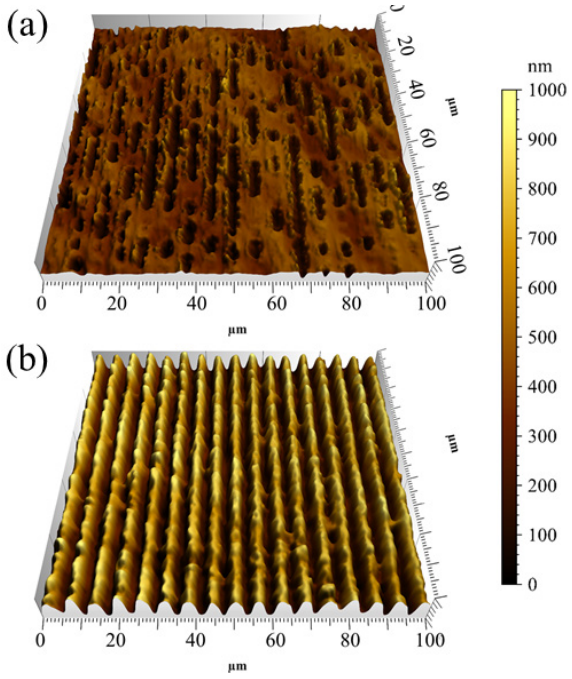

Fig. 2 WLI images of DLIP line-like structures at the central region of the elongated spot produced at (a) 0.69 J/cm² and (b) 1.39 J/cm² on additive manufactured Ti-6Al-V alloy samples.

Likewise, the Scancromal® samples were also irradiated using single laser pulses at different fluence levels, presenting a behavior that shows some difference with the Ti surfaces. In the low fluence range, from 0.25 to ~0.8 J/cm², the periodic grooves had an average structure depth below 200 nm (see Figure 4) and the structure depth did not show a significan increase with higher laser fluences. At a fluence level of ~0.85 J/cm², the structure depth starts to increase until it saturates when the energy density surpasses 1.20 J/cm². In addition, the maximal depth reached with a single laser pulse for this material was higher than for the Ti-6Al-V sample when using the same energy levels. For example, at a laser fluence of 1.39 J/cm², the structure depths were 659 ± 57 and 1129 ± 159 nm for the Ti and Al alloys, respectively.

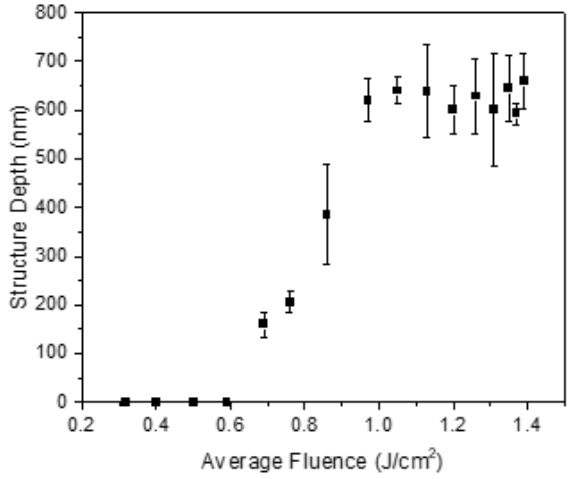

Fig. 3 Variation of structure depth with applied laser fluence in Ti-6Al-V alloy.

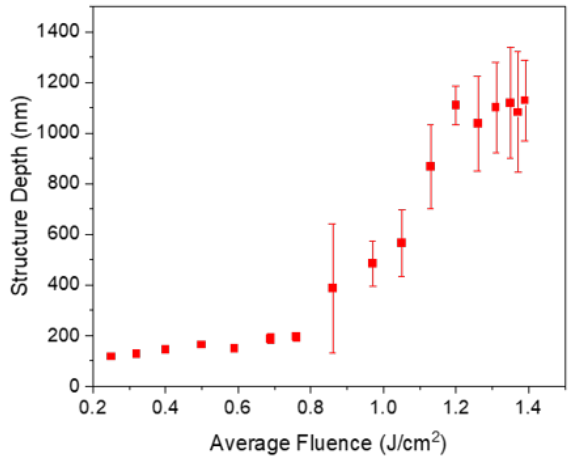

Fig. 4 Variation of structure depth with applied laser fluence in Scancromal®.

Exemplary WLI images of the DLIP treated Scancromal® samples are shown in Figure 5 for laser fluences of 0.69 J/cm² and 1.39 J/cm². From the images, it can be noticed that shallow periodical ripples are present in the sample surface. For this experiment held at 0.69 J/cm² the topography shows less irregularities than the experiment held at same fluence in Ti-6Al-4V (Figure 2a). In contrast, for the structuring experiment held at 1.39 J/cm² it can be seen that the quality of the periodic structures decreases. A similar behavior has previously been observed for structures fabricated in aluminium with a period of 5 µm and similar fluence. According to the findings stated in [39], the decrease in the quality of the pattern can be attributed to the turbulent flow occurring in the molten aluminium pool (high Marangoni number) at the beginning of the laser-meterial interaction when the vaporization temperature is reached. Also, protrusions and irregularities along the direction of the ripple lines can be caused by instabilities in material flow induced by thermo-capillary stresses [24].

3.2 Temporal evolution during single pulse DLIP experiments

Time-resolved reflectivity (TRR) measurements were employed as a way to monitor the formation of periodic structures during a single ns-DLIP pulse. As mentioned in the introduction section, the main objective of such experiment is to obtain new insights about the dynamics of periodical structure formation on the here utilized AM materials.

As it was previously described in the experimental section, the reflectivity of the area that is being laser-treated with the two-beam DLIP configuration is simultaneously exposed to the probe laser (He:Ne). Due to the formation of the line-like periodic surface pattern, the probe laser beam is diffracted and the intensity of the zero diffraction order is captured by the photodetector [35]. The variations of the TRR signal intensity that arise during the structuring process can be related to an increase of the intensity in the higher diffraction orders (±1, ±2, ±3, etc), which results in a reduction of the intensity for the zero order [35]. In addition, temperature changes at the material surface can also affect the material reflectivity [31].

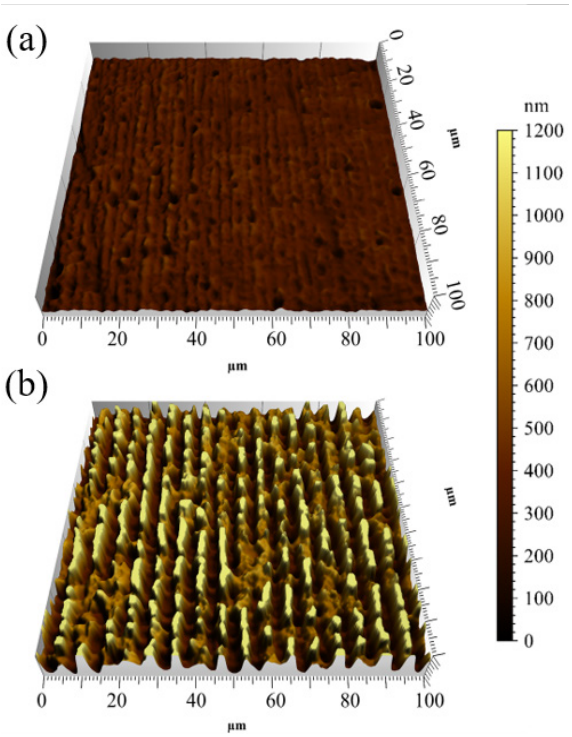

Fig. 5 WLI of DLIP line-like structures at the central region of the elongated spot produced at (a) 0.69 mJ/cm², (b) 1.39 J/cm² on additive manufactured Scancromal®.

Exemplary TRR curves obtained at laser fluences of 0.40 J/cm², 0.69 J/cm² and 1.39 J/cm² are presented in Figure 6a for the used Ti-alloy. The photodiode output curves were analyzed by utilizing the method previously described in [34], where a 100-point FFT filter was applied to the raw signal to reduce the high-frequency noise. The intensity variation of the reflected zero order was deduced from the voltage difference (ΔV) between the initial state (before the pulse was fired) and the final or steady state.

On the temporal axis, a first breakage in the reflectivity curve denotes the beginning of the melting process. The end of the re-solidification process is characterized by an inflection point in the curve following the signal's minimum, as reported in previous studies for stainless steel [31]. The interval between those points represents the duration in which the material remains in the molten state (melting time). Although the exact laser firing time is not indicated on the curve, it is assumed to occur a few nanoseconds (2 - 4 ns for a 6 ns

laser pulse) before the steep decline in the voltage signal [32,37]. It is important to notice that the initial voltage values were not always the same due to small differences in the substrate surface or due to a deviation in the direction of the probe laser which is later captured by the photodetector.

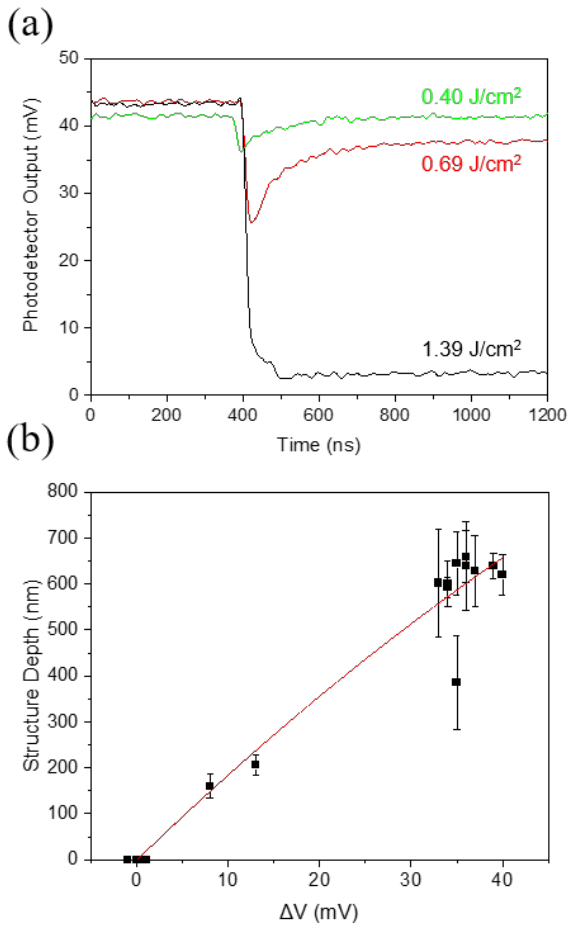

Fig. 6 (a) Time-resolved reflectivity (TRR) curves of the DLIP treated Ti-6Al-4V samples at different laser fluences. (b) Structure depth as function of the difference in starting and final voltage (intensity of the zero diffraction order) after each pulse.

The aforementioned behavior is consistently observed across various laser fluences, as shown in Figure 6a. Initially, the measured voltage represents the reflectivity of the untreated surface (approximately 40 – 45 mV). A significant voltage drop indicating substantial structural changes occurs within ~10 ns, depending on the applied laser fluence. Subsequently, the voltage further drops, suggesting also an intensity reduction of the zero diffraction order due to the formation of the periodic structure. For the lowest fluence (0.40 J/cm^2) it can be observed that a drop in the reflectivity occurs when the laser pulse is interacting with the material but after a few tens of nanoseconds, the voltage signal increases reaching values similar as before the DLIP pulse was applied. This behavior can be attributed for instance to the local increased temperature which produces a decrease in the reflectivity, as it is common for metals [31]. Thus, since at this laser fluence the periodic structure was not formed, the reflectivity almost recovered its initial value after cooling down.

For higher fluences (e.g., 0.69 J/cm², Figure 6a), the final voltage signal has a higher intensity compared to the time in which the material is molten, but also lower compared to the intensity before the DLIP laser pulse is applied. As explained before, this increase might result from temperature effects. Another effect that can explain this behavior is a reduction of the structure depth during the structuring process, as was reported for stainless steel in thermal simulations considering the dynamic of the molten material performed by Heinrich et al. [36]. In that work, it was observed that the molten material that is forming the structure topography (which flows from the intensity maxima positions) forms the periodic structure in the first hundreds of ns, reaching a maximal depth and after that the depth of the structure decreases due to gravity or changes in the material's density when it changes from the liquid to the solid phase.

On the other hand, at higher laser fluences a different behavior was observed. The TRR curve of the material irradiated at 1.39 J/cm² follows the same behavior at the beginning of the process, but once the lowest intensity of the zero diffraction order (voltage) is reached, the intensity of the signal remains constant. A possible explanation to this phenomenon is that for these fluence levels, the amount of laser intensity (of the probe laser) going into the higher orders of diffraction surpases is dominant compared to the temperature effects.

In case of the laser fluence range between 0.69 and 1.39 J/cm², melting times between 128 and 162 ns were determined as indicated in Table 1. This approach has been previously used for stainless steel, calculating times in the range from 73 to 380 ns, for laser fluences between 1.9 and 5.9 J/cm² which are similar to the values here reported [34].

Table 1 Calculated melting times and maximal growth rates

Ti-6Al-4V Fluence (J/cm²)	Melting time (ns)	Maximal growth rate (nm/ns)
0.69 J/cm²	128 ± 19	~18
0.87 J/cm²	145 ± 46	~35
1.39 J/cm²	162 ± 19	~35
Scancromal Fluence (J/cm²)	**Melting time (ns)**	**Maximal growth rate (nm/ns)**
0.32 J/cm²	62 ± 10	~25
0.69 J/cm²	107 ± 14	~45
1.39 J/cm²	115 ± 22	~50

Finally, a correlation between the voltage variation (ΔV) and the structure depths of the DLIP-treated samples (measured with WLI after the process) for all applied fluences was calculated, as shown in Figure 6b. It is noted that at higher laser fluences, where larger structure depths are obtained, significant changes in the zero diffraction order intensity arise. This effect is in agreement with previous research studies regarding the fabrication of periodic patterns using DLIP with ns-pulses [35].

A polynomial fit was then applied for the data in Figure 6b, yielding an R^2 of 0.97. This fitting model was employed to calculate the evolution of the structure depth in single-pulse ns-DLIP experiments as function of time. To simplify the model, the temperature's impact on reflectivity was neglected. Thus, variations in zero diffraction order intensities were solely attributed to changes in structure depth induced by the line-like topography (diffraction grating) formed on

the Ti-6Al-4V surface. The time-dependent structure depth evolution is depicted in Figure 7a. From the curves, the aforementioned behaviors can be distinguished, particularly the retraction in the structure depth for a laser fluence of 0.69 J/cm².

Furthermore, since the curve's slope indicates the velocity of structure growth, the first derivative of the structure depth was calculated and plotted in Figure 7b. From this calculations, a maximum growth rate of ~35 nm/ns was found for the highest fluence (1.39 J/cm²). In turn, for a lower fluence of 0.69 J/cm², the velocity of structure growth reaches 18 nm/ns. Due to the retraction of the DLIP-induced ridges produced at the fluence of 0.69 J/cm², a negative growth rate up to -2.5 nm/ns was estimated after 50 ns of the triggering of the structure formation. However, since the effect of the temperature in the reflectivity was neglected, this negative rate can not be assured and require further investigations.

Time resolved reflectivity curves for Scancromal® samples (Figure 8a) show a similar behavior than the experiments performed in the titanium samples. Firstly, for the lowest used fluence (0.40 mJ/cm^2), it can be noticed that the voltage drops approximately at 400 ns and after a steep decrease, the intensity of the zero diffraction order slowly starts to recover to a value below the initial reflectivity. This indicates a permanent change in the surface topography. Later, the curves show a steeper "V" shape than the experiments performed for the titanium-alloy samples. Similarly as for the Ti-samples, for the highest fluence of 1.39 J/cm², only a minimal recovery of the reflectivity can be noticed.

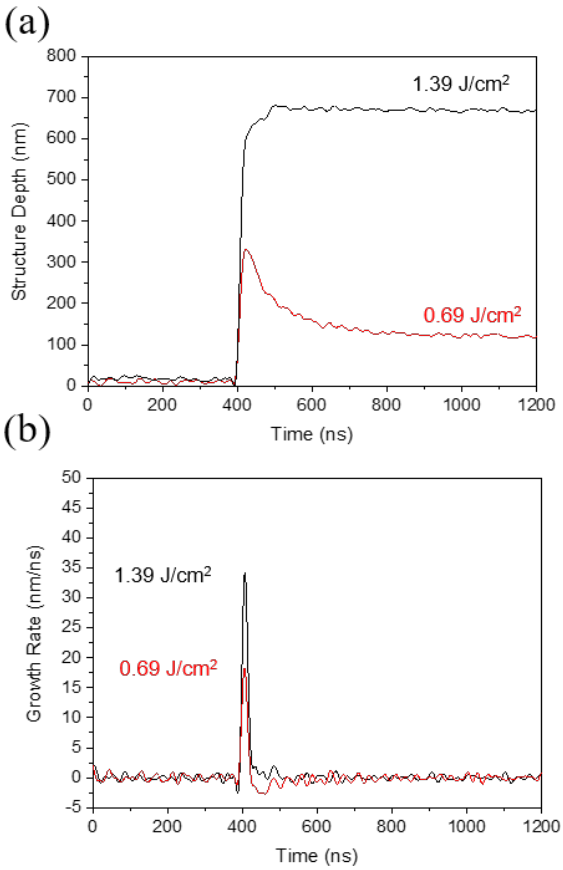

Fig. 7 (a) Time-resolved variation of structure depth during a single laser pulse in Titanium, (b) Structure growth rate obtained as the 1st derivative of the time resolved structure depth variation.

From the above presented results, melting times of 62 ± 11 ns (for 0.32 mJ/cm^2) and 115 ± 22 ns (for 1.39 J/cm^2) could be calculated from the curves which are shorter compared to Ti-6Al-4V. This values are indicated also in Table 1. This behaviour can be attributed to the significantly higher thermal conductivity for Scancromal, which means that the heat is faster dissipated to the bulk of the material and thus the molten material can solidify faster.

Also in this case, a comparative analysis between the intensity variation of the zero diffraction order (ΔV) and the structure depth was performed (Figure 8b). As for the previous material, it can be seen that periodic surfaces having more pronounced changes in zeroth diffraction order intensity are related to deeper structures. This data was also fitted with a polynominal fit yielding a coefficient R^2 of 0.98.

The polynominal fit was then used to estimate the time-resolved evolution of the structure depth, as shown in Figure 9a. Also in this case, the influence of the temperature in the reflectivity of the material was neglected for a simplification of the model.

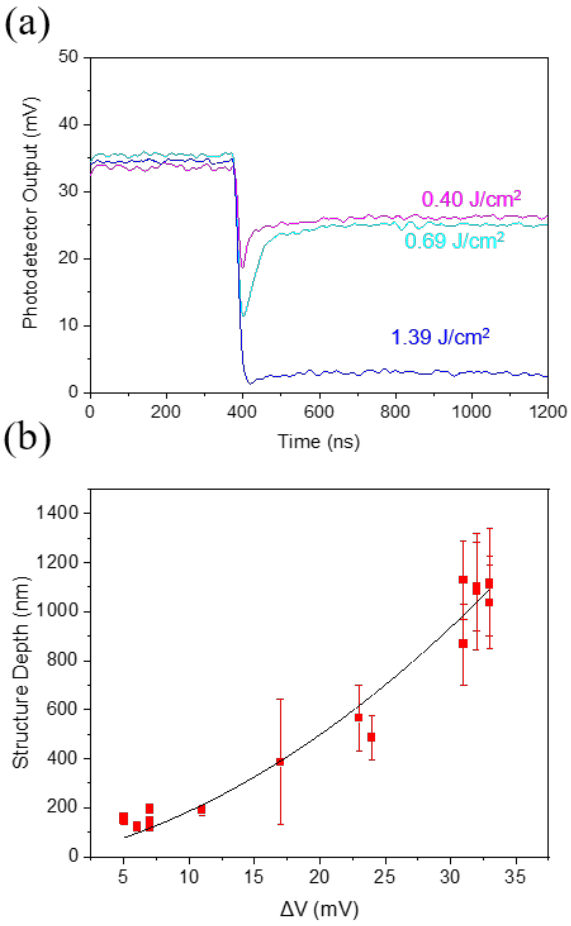

Fig. 8 (a) Time-resolved reflectivity curves of Scancromal® samples irradiation at different laser fluences, (b) Difference in starting and final reflectivity (voltage) after each pulse as function of structure depth in Scancromal®.

The obtained results show a similar behaviour as the ones calculated for titanium (and also for stainless steel in [34]). However, due to the relative shorter melting times as well as the deeper structures obtained compared to Ti-6Al-4V, higher growth rates occur (see Figure 9b and Table 1). For example, at 1.39 J/cm², a growth rate of ~50 nm/ns was

observed for this material (Scancromal®) in contrast of the ~35 nm/ns for Ti, which is approximately 43 % higher (at the same laser fluence). This faster speed can also be attributed to the difference in viscosity at molten state of both materials. Although Scancromal® thermochemical properties have not been thoroughly reported, the viscosity of pure aluminium in the molten state is known to be in the range of 1.0 to 1.4 mPa.s [40]. On the other hand, the titanium alloy under study exhibits a viscosity of around 4.76 mPa.s at melting temperatures, as reported by [41]. Thus, the lower viscosity of Scancromal® could enable a faster material flow from the interference maxima to minima positions and therefore a faster structure growth rates.

Although this method has shown to be efficient to estimate the dynamics of structure formation when using ns-pulses in DLIP [34], the effect of surface temperature has to be considered in the model for better accuracy. Nevertheless, the results presented here have allowed for a quantitative differentiation of the structure formation dynamics in metallic substrates with significantly different thermal properties. This has enabled a deeper understanding of the formation of periodic structures in metals when they are trated by ns-DLIP single pulses.

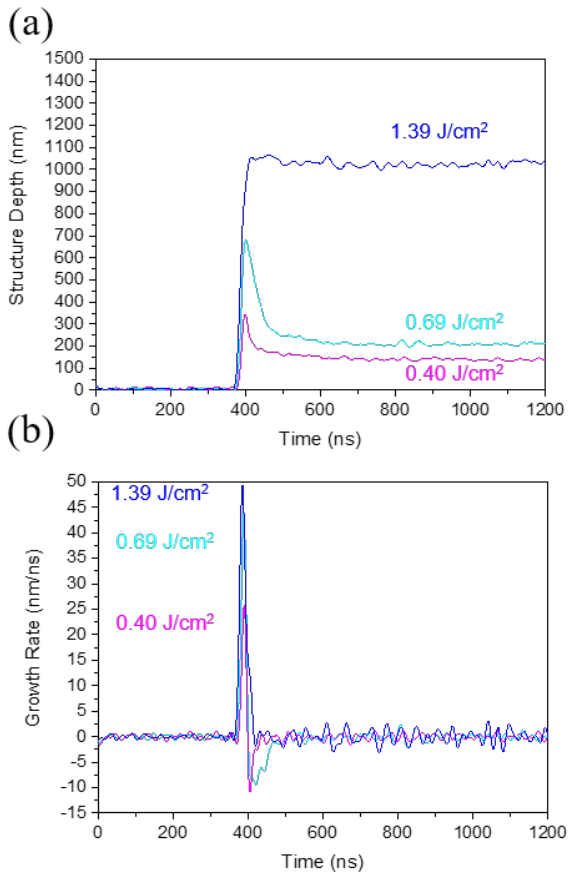

Fig. 9 (a) Time-resolved variation of structure depth during a single laser pulse in Scancromal®, (b) Structure grow rate obtained as the 1st derivative of the time resolved structure depth variation.

4. Conclusions

An optical probing method was employed to monitor the Direct Laser Interference Patterning process on Ti-6Al-4V and Scancromal® alloys. Single laser pulses (6 ns) with fluences ranging from 0.18 J/cm² to 1.39 J/cm² were employed to produce periodic line-like structures. Time-resolved reflectivity measurements were used for the experimental assesment of material dynamics during single pulse ns-DLIP processes as well as to calculate the growth rates during the formation of the structures. The key findings of this study can be summarized in:

I. The melting times in ns-DLIP increased with laser fluence. For Ti-6Al-4V, it ranged from 128 ns to 154 ns, while for Scancromal® they were shorter, varying from 62 and 115 ns for laser fluences between 0.32 J/cm² (0.69 J/cm² fot Ti) and 1.39 J/cm², respectively.
II. Variations in temporal evolution allowed the estimation of the growth rates of the produced line-like structures, reaching values up to ~35 nm/ns and ~50 nm/ns for Ti-6Al-4V and Scancromal®, respectively.
III. The above mentioned differences can be explained by the significantly different thermal properties as well as by the viscosity of the molten phase of the investigated materials.

This method has proven efficient for estimating structure formation dynamics with ns-pulses in DLIP, although surface temperature effects have been disregarded for simplicity. The reported results allowed identifying the structure formation dynamics in metals with varying thermal properties, enhancing the understanding of periodic structure formation in metals.

Acknowledgments

Funded by the European Union under grant 101091373. Views and opinions expressed are however those of the authors only and do not necessarily reflect those of the European Union. Neither the European Union nor the granting authority can be held responsible for them.

References

[1] J. C. Najmon, S. Raeisi, A. Tovar: "Additive Manufacturing for the Aerospace Industry" ed. by F. Froes and R. Boyer, (Elsevier, Netherlands, 2019) p.7.
[2] S. Singamneni, L. V. Yifan, A. Hewitt, R. Chalk, W. Thomas, and D. Jordison: J. Aeronaut. Aerosp. Eng., 8, (2019) 1000214J.
[3] D. Bourell, J. P. Kruth, M. Leu, G. Levy, D. Rosen, A. M. Beese, and A. Clare: CIRP Ann. Manuf. Technol., 66, (2017) 659.
[4] R. Boilatt, S. P. Isanaka, and F. Liou: Crystals, 11, (2021) 524.
[5] A. Gomez-Gallegos, P. Mandal, D. Gonzalez, N. Zuelli, and P. Blackwell: Defect Diffus. Forum, 385, (2018) 419.
[6] T. Wagner, and C. Neinhuis: Acta Zool., 77, (1996) 213.
[7] R. Helbig, J. Nickerl, and J. Neinhuis: PLOS ONE, 6, (2011) e25105.
[8] P. Ball: Nature, 400, (1999) 1.
[9] A. G. Dumanli, and T. Savin: Chem. Soc. Rev., 45, (2016) 6698.
[10] J. Minguela, D. W. Müller, F. Mücklich, L. Llanes, M.P. Ginebra, J.J. Roa, and C. Mas-Moruno: Mater. Sci. Eng.: C, 125, (2021) 112096.
[11] J. Z. Yu, E. Korkmaz, M. I. Berg, P. R. Le Duc, and O.B Ozdonganlar: Biomaterials, 128, (2017) 109.

[12] H. Shahali, J. Hasan, H.-H. Cheng, S. Ramarishna, and P. K. Yarlagadda: Nanotechnology, 32, (2020) 065301.
[13] F. Watt, A. A. Bettiol, J. A. Van Kan, E. J. Teo, and M. B. H Bresse: Nanoscience, 04, (2005) 269.
[14] A. F. Lasagni: J. Laser Micro/Nanoengenieering, 10, (2015) 340.
[15] S. Rekštytė, A. Žukauskas, V. Purlys, Y. Gordienko, and M. Malinauskas: Appl. Surf. Sci., 270, (2013) 382.
[16] F. Fraggelakis, G. D. Tsibsidis, and E. Stratakis: Phys. Rev. B., 103, (2021) 054105.
[17] D. Fabris, A.F. Lasagni, M. Fredel, and B. Henriques: Ceramics, 2, (2019) 578.
[18] D. W. Müller, T. Fox, P. G. Grützmacher, S. Suarez, and F. Mücklich: Sci. Rep., 10, (2020) 3647.
[19] A. F. Lasagni, F. Mücklich, M. R. Nejati, and R. Clasen: Adv. Eng. Mater., 8, (2006) 580.
[20] Bäuerle, D: "Laser Processing and Chemistry", (Springer Berlin Heidelberg, Germany, 1996), p.152.
[21] M. D'Alessandria, A. F. Lasagni, and F. Mücklich: App. Surf. Sci., 255, (2008) 3210.
[22] J.T. Cardoso, A.I. Aguilar-Morales, S. Alamri, D. Huerta-Murillo, F. Cordovilla, A.F. Lasagni, and J.L. Ocaña: Opt. Lasers Eng., 111, (2018) 193.
[23] J. -M. Drezet, S. Pellerin, C. Bezençon, and S. Mokadem: J. Phys. IV, 120, (2004) 299.
[24] A. F. Lasagni, M. D'Alessandria, R. Giovanelli, and F. Mücklich: App. Surf. Sci., 254, (2007) 907.
[25] S. Indrišiūnas, B. Voisiat, M. Gedvilas, and G. Račiukaitis: Journal of Micromech. Microeng., 23, (2013) 095034.
[26] A. Rank, T. Kunze, T. Hoffmann, and A.F. Lasagni: Adv. Eng. Mater., 18, (2016) 1280.
[27] R. J. Peláez, E. Rebollar, R Serna, C. Acosta-Zepeda, P. Saavedra, J. Bonse, and E. Haro-Poniatowski: J. Phys. D: App, Phys, 52, (2019) 225302.
[28] R. J. Peláez, T. Kuhn, F. Vega, and C. N. Alfonso: App. Phys. Lett., 105, (2014) 161911.
[29] J. Bonse, S. M. Wiggins, and J. Solis: App. Phys. A, 80, (2005) 243.
[30] J. Bonse, G. Bachelier, J. Siegel, and J. Solis: Phys. Rev. B, 74, (2006) 134106.
[31] J. Martan, O. Cibulka, and N. Semmar: App. Surf. Sci., 253, (2006) 1170.
[32] R. Fang, A. Vorobyev, and C. Guo: Light: Sci. Appl., 6, (2017) e16256.
[33] M. Alvarez-Alegria, C. Ruiz de Galarreta, and J. Siegel: Laser Photonics Rev., 17, (2023) 2300145.
[34] I. Tabares, M. Soldera, B. Voisiat, and A. F. Lasagni: Sci. Rep., 14, (2024) 9599.
[35] N. Schröder, C. Fischer, M. Soldera, B. Voisiat, and A. F. Lasagni: Adv. Eng. Mat., 25, (2023) 2201889.
[36] M. Heinrich, B. Voisiat, A. F. Lasagni, and R. Schwarze: PLOS ONE, 18, (2023) e0282266.
[37] Boneberg, J., Bischof, and J., Leiderer, P.: Opt. Commun., 174, (2000) 145.
[38] C. Zwahr, D. Günther, T. Brinkmann, N. Gulow, S. Oswald, M. Grosse Holthaus, and A. F. Lasagni: Adv. Healthc. Mater., 6, (2017) 1600858.
[39] M. Bieda, E. Bayer, and A. F. Lasagni: ASME. J. Eng. Mater. Technol., 132(3), (2010) 031015.
[40] A.T. Dinsdale, and P.N. Quested: J. Mater. Sci., 39, (2004) 7221.
[41] R. Wunderlich: High Temp. Mater. Process., 27(6), (2008) 401.

(Received: June 13, 2024, Accepted: October 20, 2024)